STRUCTURAL BIOLOGY

**Volume 79 (2023)**

**Supporting information for article:**

# Ambient temperature structure of phosphoketolase from *Bifidobacterium longum* determined by serial femtosecond X-ray crystallography

**Kunio Nakata, Tatsuki Kashiwagi, Naoki Kunishima, Hisashi Naitow, Yoshinori Matsuura, Hiroshi Miyano, Toshimi Mizukoshi, Kensuke Tono, Makina Yabashi, Eriko Nango and So Iwata**

**S1. Effectiveness of the light-induced crystallization for generating microcrystals**

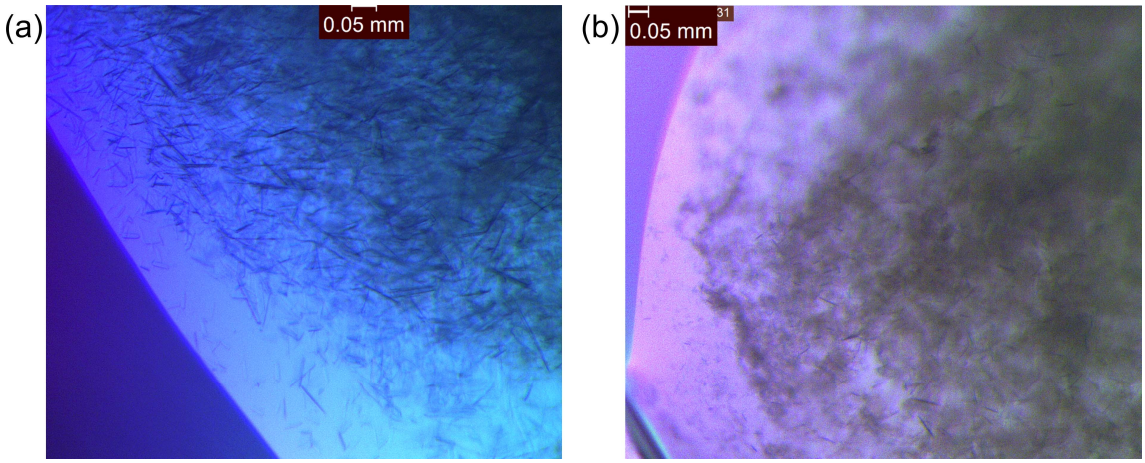


**Figure S1** . Micro-sized crystallization of *Bifidobacterium longum* phosphoketolase (BIPKT) utilizing the light-induced crystallization plate (Fujifilm Wako). The photographs were taken using an M205C microscope (Leica). (a) Incubation for one day with the irradiation of fluorescent light at 25°C. Various sized spindle shape microcrystals of BIPKT were observed. (b) Incubation for one week without the irradiation of fluorescent light at 25°C (control). Foggy precipitation of BIPKT was mainly observed.

### S2. Crystal packing of BlPKT crystals

To explore the influence of cryocooling on crystal structures, the crystal packing interactions within $BlPKT_{XFEL}$, PEP-$BlPKT_{XFEL}$, and $BlPKT_{cryo}$ structures were analyzed. As mentioned in section 3.1, the cell lengths of *a*, *b*, and *c*-axes of the $BlPKT_{cryo}$ crystal (Takahashi *et al.*, 2010) were shrunk by ≈ 1.6%, 0.7%, and 3.3%, respectively, when they were compared with those of $BlPKT_{XFEL}$ crystal. In the BlPKT crystal structures, there were three major contact regions (I, II, and III) and three minor contact regions (IV, V, and VI) between neighboring octamers (Table S1, S2).

Among the three major contact regions (Fig. S2(a)), the contact region I of each structure seemed to be significantly diverse in the crystal packing interaction (Fig. S2(b), Table S1). The contact region I mainly existed between protomer C of the original BlPKT octamer at (X, Y, Z) and protomer D of the symmetry related octamer at (-X-1, Y-1/2, -Z-1). This interaction contains the translations of *a* and *c* axis directions and may be affected by relatively large crystal shrinkage of these directions in the $BlPKT_{cryo}$ structure. The loop at V322–A332 in the protomer D formed the interface of the contact region I of BlPKT crystals (Table S1), and the conformation of this loop in the $BlPKT_{cryo}$ structure was apparently different from those in the $BlPKT_{XFEL}$ and PEP-$BlPKT_{XFEL}$ structures (Fig. 2(b) $, Fig. S3(b)). The conformation of the loop at V322–A332 in the protomer D was almost identical to those in the other seven protomers in the $BlPKT_{XFEL}$ or PEP-$BlPKT_{XFEL}$ structure, whereas it was significantly different from the other seven protomers in the $BlPKT_{cryo}$ structure. This example of structural distortion at the crystal packing interface demonstrates that the XFEL-SFX method can avoid structural artifacts using the cryogenic treatment.

Structural change due to the difference in crystal packing was also observed at minor contact region IV in the $BlPKT_{cryo}$ structure. The loop at E50–E55 in protomer B formed the interface of contact region IV of the BlPKT crystals (Table S1), and Cα atom positions in this loop of the $BlPKT_{cryo}$ structure was different from those in the $BlPKT_{XFEL}$ and PEP-$BlPKT_{XFEL}$ structures (Fig. 2(b) #, Fig. S3(a)).

The polar interactions of major contact regions II and III were relatively similar among the three BlPKT structures (Table S1). The contact regions II and III mainly existed between protomer A of the original BlPKT octamer and protomer G of the symmetry related octamer at (-X, Y-1/2, -Z), and between protomer B of the original BlPKT octamer and protomer E of the symmetry related octamer at (-X, Y+1/2, -Z), respectively. From these interactions, BlPKT octamers were positioned along the crystallographic 2-fold screw axis (*b*-axis) of the BlPKT crystal structure

(Fig. S2(a)). Because the crystal shrink of the *b*-axis was not overly large, the crystal packing interactions of contact regions II and III may not have drastically changed. These contact regions demonstrated several characteristic features. Interestingly, although contact regions II and III were crystallographically independent, the patterns of their eight polar interactions were identical within the $BlPKT_{XFEL}$ structure (Table S1). Furthermore, these contact regions contained two hydrogen bonds between acidic side chains (E55–D615 and E123–E622). They were also conserved in the $BlPKT_{cryo}$, and PEP-$BlPKT_{XFEL}$ structures, implying that these hydrogen bonds between acidic side chains played an important role in crystal packing. However, these hydrogen bonds are expected to destabilize under neutral and alkaline conditions due to deprotonation of the side chain carboxyl groups in the acidic residues. In fact, $BlPKT_{cryo}$ (Takahashi *et al.*, 2010), $BlPKT_{XFEL}$, and PEP-$BlPKT_{XFEL}$ crystals were deposited under weak acidic conditions (pH 5).

**Table S1** Crystal packing polar interactions in BlPKT crystals.

| Contact Region | Original octamer | | | Neighboring octamer | | | | Atomic distance (Å) [*1] | | |
|---|---|---|---|---|---|---|---|---|---|---|
| | Residue Name | Atom Name | Chain ID | Residue Name | Atom Name | Chain ID | Symmetry Operator | $BlPKT_{cryo}$ | $BlPKT_{XFEL}$ | PEP-$BlPKT_{XFEL}$ |
| I [*2] | R43 | Nε | C | E331 | Oε1 | D | -X-1, Y-1/2, -Z-1 | 2.70 | - | - |
| | | Nη2 | C | | Oε2 | D | -X-1, Y-1/2, -Z-1 | 3.15 | - | - |
| | S44 | Oγ | C | R54 | Nη1 | D | -X-1, Y-1/2, -Z-1 | - | 3.05 | - |
| | E50 | Oε1 | C | Y793 | Oη | C | -X-1, Y-1/2, -Z-1 | - | 3.27 | - |
| | E50 | O | C | H59 | Nδ1 | D | -X-1, Y-1/2, -Z-1 | 3.04 | 3.05 | - |
| | | O | C | | Cε1 | D | -X-1, Y-1/2, -Z-1 | 2.96 | 2.88 | - |
| | E50 | O | C | R328 | Nε | D | -X-1, Y-1/2, -Z-1 | 2.85 | - | - |
| | | O | C | | Nη1 | D | -X-1, Y-1/2, -Z-1 | 3.06 | 3.03 | - |
| | E55 | Oε1 | C | E331 | N | D | -X-1, Y-1/2, -Z-1 | 2.79 | - | - |
| | D56 | Oδ1 | C | R54 | Nη2 | D | -X-1, Y-1/2, -Z-1 | 2.85 | 3.19 | - |
| | K118 | Nζ | C | E50 | Oε1 | D | -X-1, Y-1/2, -Z-1 | - | 3.05 | - |
| | E123 | Oε2 | C | E55 | Oε2 | D | -X-1, Y-1/2, -Z-1 | - | 2.94 | - |
| | K128 | Nζ | C | E50 | Oε1 | D | -X-1, Y-1/2, -Z-1 | 2.60 | - | - |
| | R131 | Nη2 | C | E331 | Oε1 | D | -X-1, Y-1/2, -Z-1 | - | - | 3.24 |
| | | Nη2 | C | | Oε2 | D | -X-1, Y-1/2, -Z-1 | - | - | 3.18 |
| II [*3] | E392 | Oε2 | A | R43 | Nη2 | G | -X, Y-1/2, -Z | 3.04 | 3.21 | - |
| | E392 | Oε1 | A | R54 | Nη1 | G | -X, Y-1/2, -Z | 3.19 | - | 3.11 |
| | E392 | Oε1 | A | R328 | Nη2 | G | -X, Y-1/2, -Z | 2.74 | 3.13 | 3.22 |
| | | Oε2 | A | | Nη1 | G | -X, Y-1/2, -Z | 3.17 | 2.95 | 3.24 |
| | D615 | Oδ1 | A | E55 | Oε2 | G | -X, Y-1/2, -Z | 2.66 | 2.66 | 2.63 |
| | D615 | Oδ1 | A | R43 | Nη1 | G | -X, Y-1/2, -Z | 3.10 | 3.21 | 2.58 |
| | | Oδ2 | A | | Nη1 | G | -X, Y-1/2, -Z | 2.96 | 2.66 | 3.29 |
| | | Oδ2 | A | | Nε | G | -X, Y-1/2, -Z | - | - | 2.99 |
| | R618 | Nη1 | A | D56 | Oδ1 | G | -X, Y-1/2, -Z | 2.74 | 3.03 | 3.00 |
| | | Nη2 | A | | Oδ2 | G | -X, Y-1/2, -Z | 2.90 | - | 3.01 |
| | R618 | Nη2 | A | P51 | O | G | -X, Y-1/2, -Z | 2.95 | 3.00 | 3.05 |
| | E622 | Oε1 | A | E123 | Oε1 | G | -X, Y-1/2, -Z | 2.62 | 2.67 | 2.72 |
| | | Oε1 | A | | Oε2 | G | -X, Y-1/2, -Z | 3.05 | 3.10 | - |
| | | Oε2 | A | | Oε1 | G | -X, Y-1/2, -Z | 3.01 | - | - |
| | N807 | Nδ2 | A | E783 | Oε2 | H | -X, Y-1/2, -Z | - | 3.27 | - |
| | K810 | Nζ | A | E783 | Oε2 | H | -X, Y-1/2, -Z | 2.94 | - | - |
| III [*3] | E392 | Oε2 | B | R43 | Nη2 | E | -X, Y+1/2, -Z | - | 3.14 | - |
| | E392 | Oε1 | B | R54 | Nη1 | E | -X, Y+1/2, -Z | 3.24 | - | - |
| | E392 | Oε1 | B | R328 | Nη2 | E | -X, Y+1/2, -Z | 2.78 | 2.95 | 3.21 |
| | | Oε2 | B | | Nη1 | E | -X, Y+1/2, -Z | - | - | 3.29 |
| | D615 | Oδ1 | B | E55 | Oε2 | E | -X, Y+1/2, -Z | 2.85 | 2.62 | 2.74 |
| | D615 | Oδ1 | B | R43 | Nη2 | E | -X, Y+1/2, -Z | - | 2.95 | 2.72 |
| | | Oδ2 | B | | Nε | E | -X, Y+1/2, -Z | - | 2.66 | 2.85 |
| | | Oδ2 | B | | Nη2 | E | -X, Y+1/2, -Z | - | 3.22 | 2.88 |
| | R618 | Nη1 | B | D56 | Oδ1 | E | -X, Y+1/2, -Z | 2.68 | 2.92 | 2.86 |
| | | Nη2 | B | | Oδ2 | E | -X, Y+1/2, -Z | 3.06 | - | - |

| | | | | | | | | | | |
|---|---|---|---|---|---|---|---|---|---|---|
| | R618 | Nη2 | B | P51 | O | E | -X, Y+1/2, -Z | 2.98 | 2.91 | 3.00 |
| | E622 | Oε1 | B | E123 | Oε1 | E | -X, Y+1/2, -Z | 2.62 | 2.68 | 2.25 |
| | | Oε1 | B | | Oε2 | E | -X, Y+1/2, -Z | 3.01 | - | - |
| | | Oε2 | B | | Oε1 | E | -X, Y+1/2, -Z | 3.11 | - | - |
| | N807 | Nδ2 | B | E783 | Oε2 | F | -X, Y+1/2, -Z | - | 2.88 | - |
| IV | R54 | Nη2 | B | E55 | Oε1 | H | X+1, Y, Z | 3.18 | - | - |
| V | K121 | Nζ | D | D638 | Oδ2 | F | -X, Y+1/2, -Z-1 | 2.53 | - | - |
| | N353 | Nδ2 | D | E693 | Oε2 | F | -X, Y+1/2, -Z-1 | - | - | 2.81 |
| VI | D809 | Oδ2 | D | K593 | Nζ | G | -X-1, Y-1/2, -Z-1 | - | 2.74 | - |

*1. Polar interactions with distance <3.3 Å are listed.

*2. Four polar interactions observed in the contact region I of the $BlPKT_{XFEL}$ structure disappeared in the $BlPKT_{cryo}$ structure and the other four polar interactions emerged within it. In the contact region I of the PEP-$BlPKT_{XFEL}$ structure, only one salt-bridge interaction between the side chains of R131 in the protomer C of the original BlPKT octamer and E331 in the protomer D of the symmetry related octamer existed, which was not conserved in the $BlPKT_{cryo}$ and $BlPKT_{XFEL}$ structures.

*3. More than half of the polar interactions in the contact regions II and III of the $BlPKT_{XFEL}$ structure were conserved in those of $BlPKT_{cryo}$ and PEP-$BlPKT_{XFEL}$ structures.

**Table S2** Crystal packing contact areas in BlPKT crystals.

| Contact Region | Original octamer | Neighboring octamer | | Contact area (Å$^2$) | | |
|---|---|---|---|---|---|---|
| | Chain ID | Chain ID | Symmetry Operator | BlPKT$_{cryo}$ | BlPKT$_{XFEL}$ | PEP- BlPKT$_{XFEL}$ |
| I | C, D | D, C | -X-1, Y-1/2, -Z-1 | 497.0 | 493.1 | 327.1 |
| II | A | G, H | -X, Y-1/2, -Z | 770.0 | 735.9 | 753.7 |
| III | B | E, F | -X, Y+1/2, -Z | 784.2 | 734.5 | 761.1 |
| IV | A, B | G, H | X+1, Y, Z | 209.9 | 92.0 | 87.5 |
| V | D | F | -X, Y+1/2, -Z-1 | 172.3 | 0.0 | 79.9 |
| VI | D | G | -X-1, Y-1/2, -Z-1 | 115.7 | 59.6 | 48.1 |

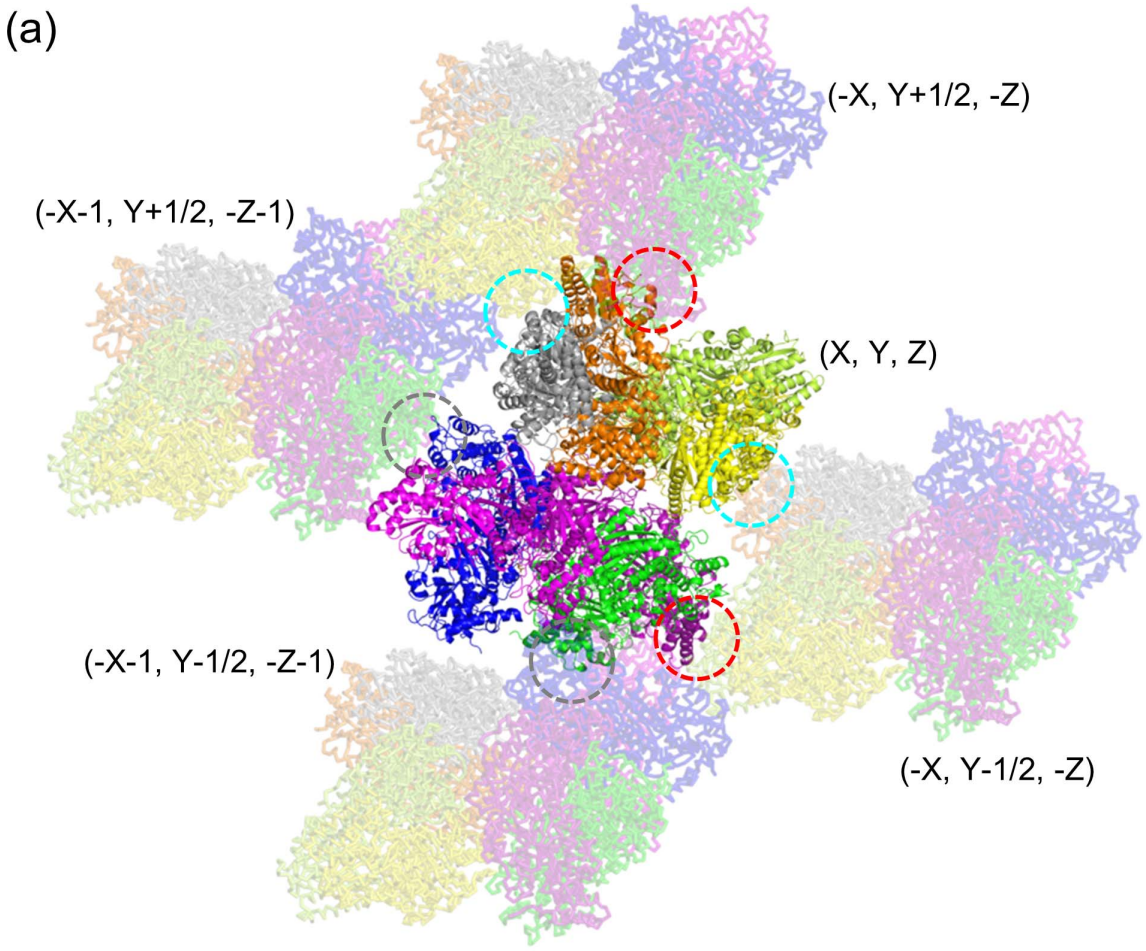
(a)
(-X, Y+1/2, -Z)
(-X-1, Y+1/2, -Z-1)
(X, Y, Z)
(-X-1, Y-1/2, -Z-1)
(-X, Y-1/2, -Z)

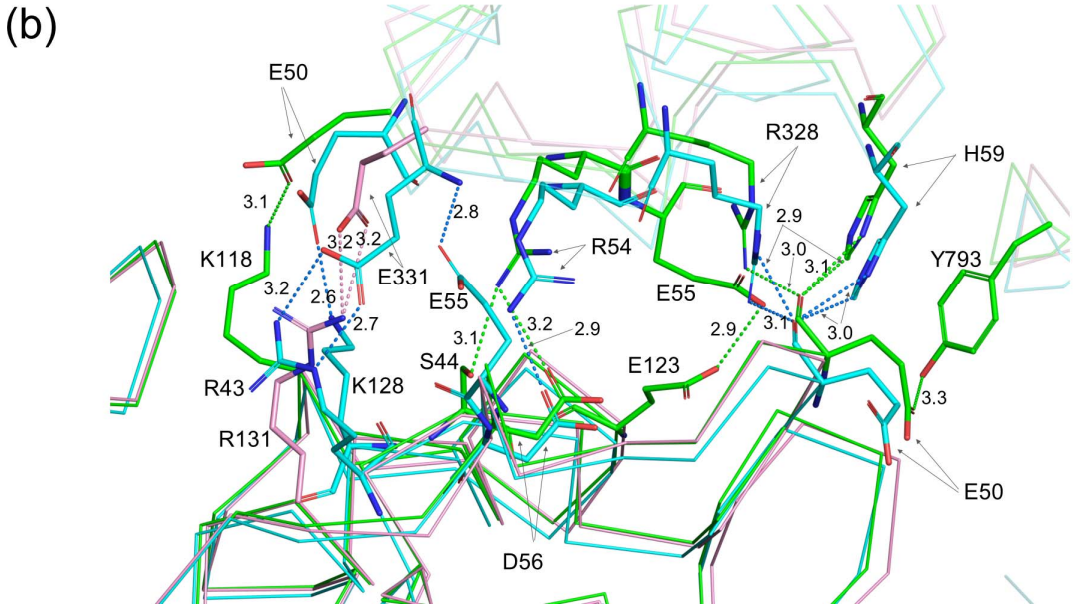
(b)
E50
R328
H59
K118
E331
R54
E55
Y793
S44
E123
R43
K128
R131
D56

**Figure S2** Crystal packing of *Bifidobacterium longum* phosphoketolase (BlPKT) crystals. (*a*) Overall view of crystal packing of the BlPKT holoenzyme structure solved by serial femtosecond crystallography ($BlPKT_{XFEL}$ structure). Ribbon models of five BlPKT octamers are shown with their symmetry operators. Octamers except for the original positioned at (X, Y, Z) are drawn with 0.7 transparency. Each protomer is colored as per Fig. 2(a). The major contact regions I, II, and III (Table S1, S2) are clarified with gray, blue, and red dotted circles, respectively. (*b*) Crystal packing interactions within the contact region I (Table S1). The Cα trace models of the original dimer CD at (X, Y, Z) and the symmetry related dimer CD at (-X-1, Y-1/2, -Z-1) are demonstrated on the bottom side with full transparency and on the top side with 0.7 transparency, respectively. The packing interaction models of the BlPKT holoenzyme structure solved by cryogenic X-ray crystallography (PDB entry 3ai7; Takahashi *et al.*, 2010), the $BlPKT_{XFEL}$ structure, and the BlPKT/phosphoenol pyruvate (PEP) complex structure solved by serial femtosecond crystallography are colored blue, green, and pink, respectively, and are superimposed with the original dimer CD. The side chains of the amino acid residues which participate in the polar interactions of each structure (Table S1) are drawn by stick models.

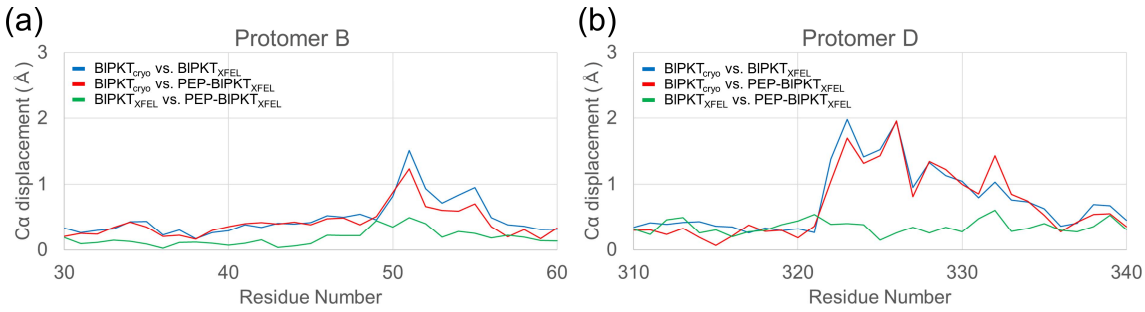


**Figure S3** Displacements of Cα coordinates between the *Bifidobacterium longum* phosphoketolase (BlPKT) structures at the regions effected by the crystal packing. Two out of three BlPKT structures (the BlPKT holoenzyme structure solved by serial femtosecond crystallography [BlPKT$_{XFEL}$ structure], the BlPKT/phosphoenol pyruvate [PEP] complex structure solved by serial femtosecond crystallography [PEP-BlPKT$_{XEFL}$ structure], and the BlPKT holoenzyme structure solved by cryogenic X-ray crystallography [PDB entry 3ai7; Takahashi *et al.*, 2010] [BlPKT$_{cryo}$ structure]) are selected and superimposed using all Cα coordinates. (*a*) Magnified view of Cα displacements around the crystal packing contact region IV of the protomer B (Fig. 2(b) #, Table S1). (*b*) Magnified view of Cα displacements around a part of the crystal packing contact region I of the protomer D (Fig. 2(b) $, Table S1).